

# Blast design for explosive demolition of a large-scale concrete foundation

Hoon Park<sup>\*†</sup>, Hyeong-Ki Park<sup>\*\*</sup>, Jin-Hee Ko<sup>\*\*</sup>, and Chul-Gi Suk<sup>\*\*</sup>

<sup>\*</sup>Chonbuk National University, 664-14 Duckjin-dong, Duckjin-gu, Jeonju, 561-756, KOREA

Phone +82-63-270-2358

<sup>†</sup>Corresponding address : hujin@jbnu.ac.kr

<sup>\*\*</sup>Korea Kacoh Co., Ltd., 1087-37 Daerim-dong, Yeongdeungpo-gu, Seoul, 150-070, KOREA

Received : November 14, 2011 Accepted : July 9, 2012

## Abstract

With the deterioration and functional loss of structures, there is an increasing demand for demolition and various demolition technologies have been developed. In case of large-scale concrete, application of some mechanical demolition techniques is limited because of the structural characteristics, and explosive demolition or explosive demolition combined with mechanical demolition is applied recently due to the effect to the surrounding environment by the ground vibration.

In this study, we compared peak particle velocity (PPV) of ground vibration depending on average fragment size ( $D_{av}$ ) in case of explosive demolition design for large-scale concrete foundation using the relation among specific charge ( $S_c$ ), charge constant ( $K$ ), and transmitting medium constant ( $n$ ) as well as the relation between average concrete fragment size ( $D_{av}$ ) and specific charge ( $S_c$ ).

**Keywords** : concrete foundation, explosive demolition, fragmentation, ground vibration.

## 1. Introduction

With the functional and structural deterioration, there is an increasing demand for demolition of industrial structures. Mechanical demolition techniques using large breaker, crusher, and diamond wire saw (D.W.S) have been applied to the demolition of industrial structures in usual. With the increasing demand for demolition, various demolition techniques have been developed and applied to control environmentally hazardous factors. There is an increasing application of explosive demolition technique that minimizes the temporal and spatial hazardous factors generated when applying mechanical demolition and considers the constructability and economic feasibility.

Among industrial structures, large-scale concrete foundation has the structural characteristics of large scale, high strength and high rigidity and thus application of some mechanical demolition techniques is limited. There is an increasing application of explosive demolition or explosive demolition combined with mechanical demolition to large scale concrete foundation demolition for the purpose of increasing the working efficiency. In addition, explosive demolition of concrete foundation accounts for

31.4% (16 cases) of explosive demolition of the civil structure that was recently performed in Korea and the number of explosive demolition is expected to increase continuously<sup>1)</sup>. The effect of ground vibration should be particularly taken into account because most large-scale concrete foundations are underground structures making a direct contact with the ground foundation.

Various studies have been conducted on ground vibration with respect to rock blasting in which the ground is drilled, but the study on the ground vibration in blast of concrete foundation near to ground foundation is not sufficient. Various models have been developed to predict and analyze the fragment size in rock blasting, and they have been applied to actual blasting sites, analyzing various blast conditions<sup>2)-6)</sup>. However, the fragment size in concrete blasting was analyzed by simply comparing the area ratios of before and after blasting in a small-scaled model<sup>7)</sup>, and the particle size distribution has not been interpreted yet.

Therefore, to provide the fundamental data for the design of large-scale concrete foundation explosive demolition in this study, we compared peak particle

**Table 1** The explosive demolition design patterns of concrete foundation for each type.

Classification	I	II	III	IV	V
Dimension ( $L \times W \times H$ , m)	2.5×2.5×1.04				
Volume ( $V$ , m <sup>3</sup> )	6.5				
Borehole diameter ( $d$ , mm)	38				
Number of holes ( $N_h$ , ea)	4				
Borehole length ( $l$ , m)	0.55	0.55	0.65	0.60	0.65
Length of charge ( $l_{ch}$ , mm)	126	168	210	250	250
Length of stemming ( $l_s$ , mm)	424	382	440	350	400
Spacing ( $S$ , m)	0.9	0.9	1.0	1.0	1.1
Burden ( $B$ , m)	0.80	0.80	0.75	0.75	0.70
Charge per hole ( $H_c$ , kg)	0.15	0.20	0.25	0.30	0.30
Specific charge ( $S_c$ , kg m <sup>-3</sup> )	0.379	0.505	0.513	0.667	0.599
Total mass of charge ( $T_c$ , kg)	0.6	0.8	1.0	1.2	1.2

velocity (PPV) of ground vibration depending on average fragment size ( $D_{av}$ ) using the relation among specific charge ( $S_c$ ), charge constant ( $K$ ) and transmitting medium constant ( $n$ ) as well as the relation between average concrete fragment size ( $D_{av}$ ) and specific charge ( $S_c$ ).

**2. Experimental method**

Concrete blasting was performed on five concrete foundations of the same scale, varying the specific charge. The average compressive strength of the concrete foundations was 21.8 MPa. Table 1 shows the design pattern of each type. Figure 1 and 2 show the design floor plans and the cross sections of the concrete foundations.

Four holes were drilled for each type using a manual rock drill. The used explosive was MegaMEX, an emulsion type explosive, of which average detonation velocity is 6,000m s<sup>-1</sup> and diameter of cartridge is 32mm. The used detonator was HiDETO Plus, an instantaneous electric detonator. The four holes of each type were ignited simultaneously. To prevent scattering of concrete fragments, a tire mat of 2.5m × 6.0m was used to cover the top and sides of the blast target concrete foundation for protection.

Figure 3 shows the location drawing of ground vibration measurement positions. The measurement positions for TYPE I, TYPE II and TYPE III were MP1 to MP6. In the

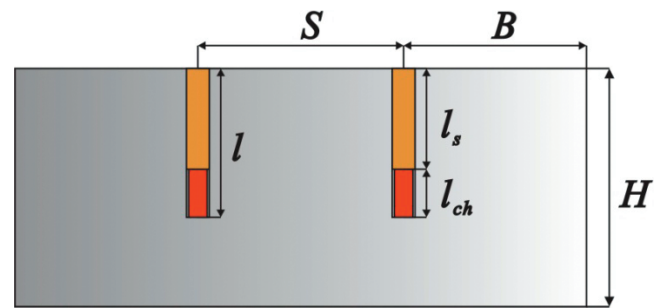


**Figure 2** The design cross section of concrete foundation.

cases of TYPE IV and TYPE V, the measurement position MP5 was moved to the MP7 position and the rest of the measurement positions were the same with those of TYPE I, TYPE II and TYPE III. A linear regression analysis was performed on the measured data to derive the prediction equation of ground vibration for each type.

After the blast, images of the concrete foundation fragment were taken for each type. To compare the concrete foundation fragment size depending on the specific charge, the average fragment size was analyzed using WipFrag software, the particle size analysis software.

**3. Results and discussion**

**3.1 Ground vibration**

Table 2 shows the ground vibration measurements of each type. Six data were acquired for each type, and thus the total number of the data was 30. The distance from the center of the blasted concrete foundation to the measurement points was 5 m ~ 56.3 m. The PPV of each composition among the entire data was 13.60 mm s<sup>-1</sup> at the distance of 5 m, which is the nearest measurement position and 0.44 mm s<sup>-1</sup> at the distance of 56.3 m, which is the farthest measurement position.

Figure 4 shows the PPV of each type and the linear regression curve of 50% according to the square-root scaled distance (SRSD). The range of the charge constant,  $K$ , was 134.3-384.1, and that of the transmitting medium constant,  $n$ , was -1.23-1.71. The  $K$  for the entire data was 206.4 and that of the  $n$  was -1.42.

Figure 5 shows the comparison between the  $S_c$  and the

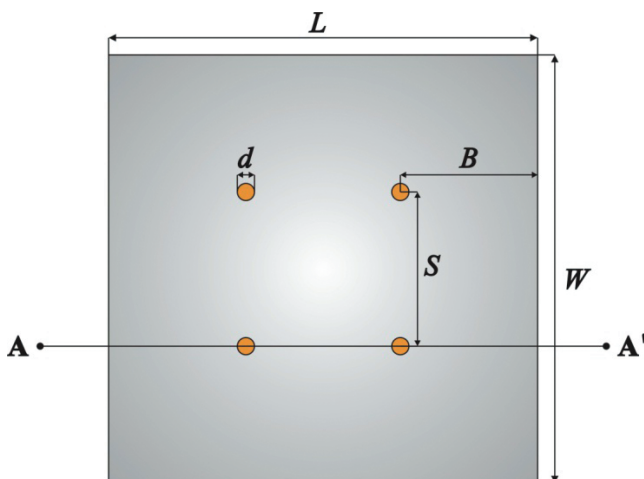


**Figure 1** The design floor plan of concrete foundation.

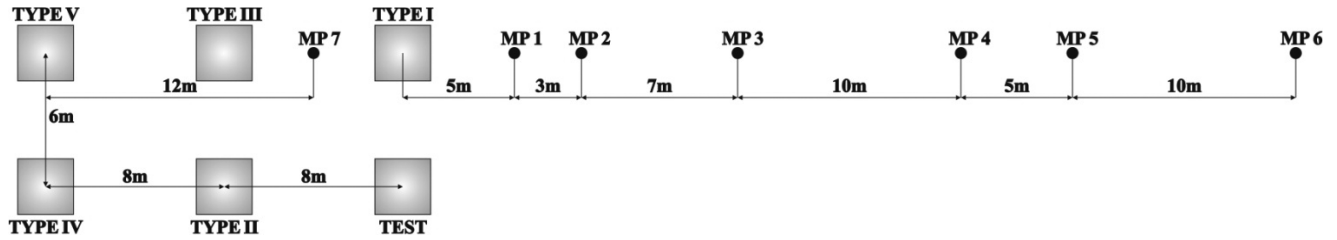


Figure 3 Ground vibration measurement positions.

Table 2 The measured PPV of ground vibration for each type.

TYPE	Measuring point	Distance [m]	Delay charge [kg]	Tran. [mm s <sup>-1</sup> ]	Vert. [mm s <sup>-1</sup> ]	Long. [mm s <sup>-1</sup> ]
I	MP1	5.0	0.6	7.95	13.10	13.60
	MP2	8.0	0.6	6.40	2.54	3.24
	MP3	15.0	0.6	4.76	1.65	3.91
	MP4	25.0	0.6	2.52	0.51	1.14
	MP5	30.0	0.6	0.91	0.71	0.94
	MP6	40.0	0.6	1.14	0.48	0.81
II	MP1	14.3	0.8	4.70	3.22	4.11
	MP2	17.1	0.8	2.27	0.89	3.06
	MP3	23.8	0.8	2.60	0.68	2.59
	MP4	33.5	0.8	1.54	0.49	1.48
	MP5	38.5	0.8	0.75	1.05	0.92
	MP6	48.4	0.8	0.76	0.67	0.70
III	MP1	13.0	1.0	1.51	4.73	5.81
	MP2	16.0	1.0	0.97	1.00	4.32
	MP3	23.0	1.0	1.21	0.62	2.91
	MP4	33.0	1.0	1.05	0.51	1.71
	MP5	38.0	1.0	0.57	1.05	0.97
	MP6	48.0	1.0	0.67	0.70	1.00
IV	MP7	13.4	1.2	3.51	3.43	6.22
	MP1	21.8	1.2	1.87	0.98	1.65
	MP2	24.7	1.2	1.41	0.35	1.48
	MP3	31.6	1.2	0.98	0.40	1.48
	MP4	41.4	1.2	0.59	0.21	0.83
	MP6	56.3	1.2	0.41	0.37	0.44
V	MP7	12.0	1.2	7.64	5.52	9.21
	MP1	21.0	1.2	1.87	1.44	2.89
	MP2	24.0	1.2	1.24	0.38	1.68
	MP3	31.0	1.2	1.30	0.48	1.79
	MP4	41.0	1.2	0.83	0.25	1.32
	MP6	56.0	1.2	0.75	0.60	0.68

$K$  and between the  $S_c$  and the  $n$  for each type. As the  $S_c$  was increased, the  $K$  was increased but the  $n$  was decreased. Thus, the tendency was that the PPV was increased as the  $S_c$  was increased to blast the equal volume of concrete.

The following Equation (1) is the relation between the  $S_c$  and the  $K$  and Equation (2) is the relation between the  $S_c$  and the  $n$ .

$$K = -183.3 + 818.6(S_c) \quad (1)$$

$$R^2 = 0.959$$

$$n = -0.598 - 1.619(S_c) \quad (2)$$

$$R^2 = 0.973$$

where  $R^2$  denotes the correlation constant.

### 3.2 Fragmentation

The fragment size distribution curve, Rosin-Rammler, used in the WipFrag software is as in Equation (3):

$$F(X) = 1 - \exp\left[-\left(\frac{X}{X_c}\right)^N\right] \quad (3)$$

where  $F(X)$  denotes the ratio of passing the screen of the size  $X$ ,  $X$  the size of the screen,  $X_c$  the characteristic size and  $N$  the uniformity index.

With Equation (3), the fragment size distribution can be expressed and evaluated using only two parameters. The

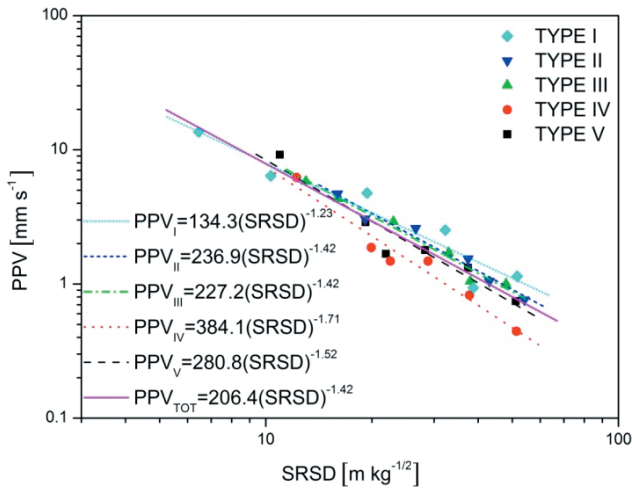


Figure 4 The relationship between PPV and SRSD for each type (50% linear regression curve).

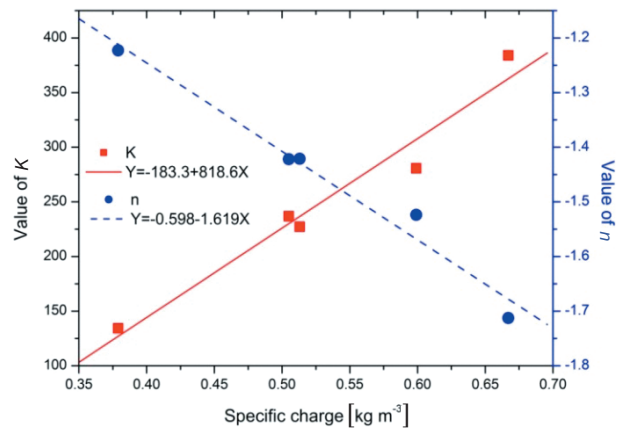
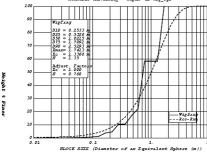
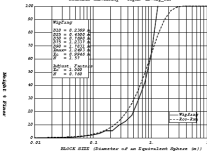
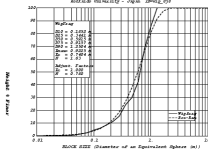
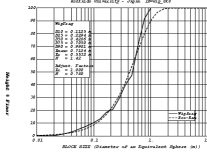
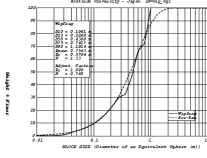


Figure 5 The relation between  $K$  and  $S_c$  and between  $n$  and  $S_c$ .

Table 3 The analytical result of the fragment size of each type.

Division	TYPE I	TYPE II	TYPE III	TYPE IV	TYPE V
Specific charge ( $S_c$ , $\text{kg m}^{-3}$ )	0.379	0.505	0.513	0.667	0.599
Fragmented concrete image					
Fragment size distribution curve					
Characteristic size ( $X_c$ , m)	1.3368	0.9948	0.7404	0.55325	0.5764
Uniformity index ( $N$ )	1.35	1.57	1.63	1.42	1.33
Average fragment size ( $D_{av}$ , m)	1.062	0.908	0.720	0.505	0.564

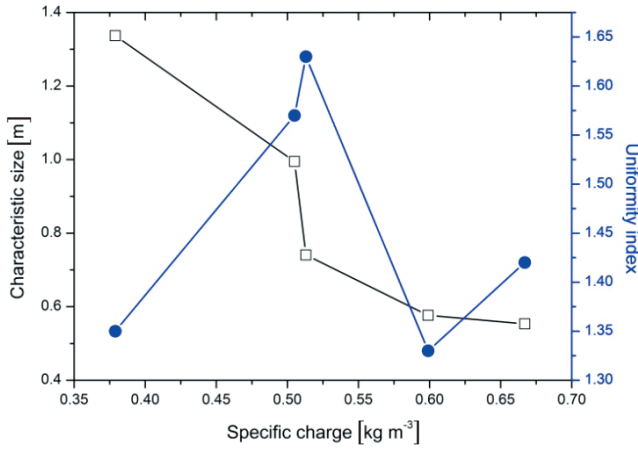
two parameters are the characteristic size ( $X_c$ ) which is the size of the screen through which 63.2% of the fragments pass and the uniformity index ( $N$ ) that determines the shape of the fragment size distribution curve (that is, the fragment size distribution characteristics).

Table 3 shows the analytical results of the fragment size of each type. The  $X_c$  was decreased as the  $S_c$  was increased, which indicated that the overall fragment size was small. The  $N$  is usually between 0.8-2.2 in case of rock blast, but it can be 0.65 depending on the burden<sup>8),9)</sup>. The  $N$  in this study was 1.33-1.63. Among the five concrete foundation samples, TYPE V showed a uniform fragment size distribution, while the fragment distribution was focused at a certain size in TYPE III. When the  $S_c$  was between 0.379 and 0.513, the  $D_{av}$  was decreased and the distribution was focused at a certain size (increased  $N$ ).

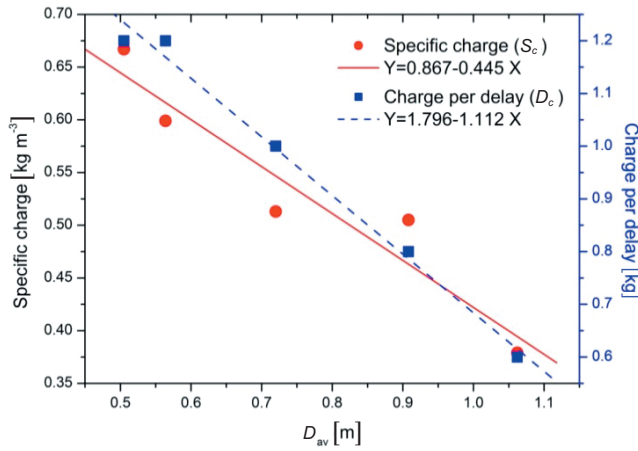
When the  $S_c$  was increased to the range between 0.513 and 0.599, the  $D_{av}$  was decreased further but the fragment size distribution became broader from small ones to the large ones (decreased  $N$ ). This might have been because some of the blasted fragments were broken to the smaller size (Figure 6).

Figure 7 shows the relation between the  $S_c$  and the  $D_{av}$  and the relation between the charge per delay ( $D_c$ ) (equal to the total mass of charge ( $T_c$ ) in this experiment) and the  $D_{av}$ . The  $D_{av}$  was decreased as the  $S_c$  and the  $D_c$  were increased. Hence, the trend was that the  $D_{av}$  was decreased as the  $S_c$  was increased to blast the equal volume concrete.

The following Equation (4) shows the relation between the  $S_c$  and the  $D_{av}$ .



**Figure 6** The relation between characteristic size and  $S_c$  and between uniformity index and  $S_c$ .



**Figure 7** The relation between  $S_c$  and  $D_{av}$  and between  $D_c$  and  $D_{av}$ .

$$S_c = 0.867 - 0.445(D_{av}) \quad (4)$$

$$R^2 = 0.915$$

### 3.3 Relation between PPV and average fragment size

In Equation (5), which is the prediction equation of ground vibration, charge per delay ( $W$ ) is the charge ignited at one hole or multiple holes simultaneously. It can be expressed as the product of  $S_c$  and the entire fragment volume of blasted concrete ( $V_f$ ) as in Equation (6). Thus, substitution of Equation (1), which is the relation between the  $S_c$  and the  $K$ , Equation (2), which is the relation between the  $S_c$  and  $n$  and Equation (4), which is the relation between the  $S_c$  and the  $D_{av}$  into Equation (6) can express the relation between PPV and the  $D_{av}$ .

$$PPV = K \left( \frac{D}{\sqrt{W}} \right)^n \quad (5)$$

$$PPV = K \left( \frac{D}{\sqrt{S_c \times V_f}} \right)^n \quad (6)$$

Figure 8 shows the relationship between PPV and distance depending on the  $D_{av}$  of 0.3 m, 0.5 m, 0.7 m and 0.9 m in the case where the entire fragment volume of blasted concrete was  $10 \text{ m}^3$ . The PPV at the distance of 10 m was  $40.48 \text{ mm s}^{-1}$  when the  $D_{av}$  was 0.3 m and  $24.95 \text{ mm s}^{-1}$  when

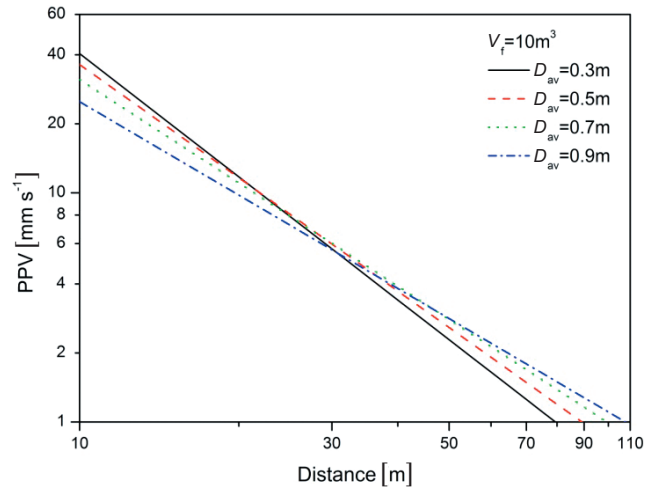


**Figure 8** The relationship between PPV and the distance depending on the  $D_{av}$  with the entire fragment volume of blasted concrete of  $10 \text{ m}^3$ .

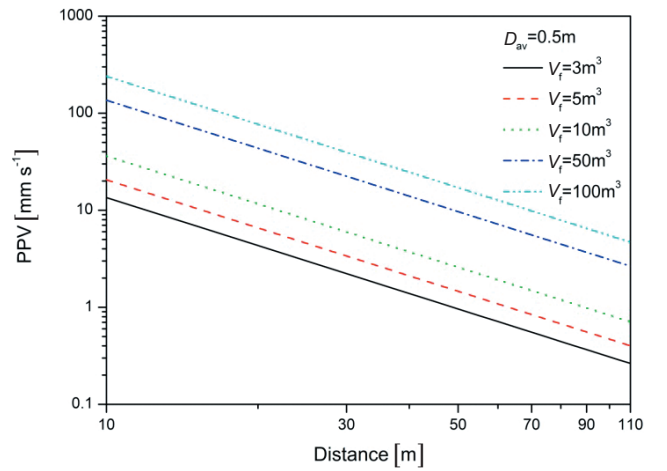


**Figure 9** The relationship between PPV and the distance depending of the entire fragment volume of blasted concrete with the  $D_{av}$  of 0.5 m

the fragment size was 0.9 m. The figure at the distance of 50 m was  $2.29 \text{ mm s}^{-1}$  and  $2.83 \text{ mm s}^{-1}$ , respectively, indicating that the PPV was greater when the  $D_{av}$  was 0.9 m. This was because  $S_c$  and  $K$  were decreased but  $n$  was increased as the  $D_{av}$  was increased when the entire fragment volume of blasted concrete was equal.

Figure 9 shows the relationship between PPV and the distance when the entire fragment volume of blasted concrete was  $3 \text{ m}^3$ ,  $5 \text{ m}^3$ ,  $10 \text{ m}^3$ ,  $50 \text{ m}^3$  and  $100 \text{ m}^3$  with the  $D_{av}$  of 0.5 m. When the  $D_{av}$  was constant, the  $n$  was also constant. However, the total mass of charge was increased and PPV was also increased as the entire fragment volume of blasted concrete was increased.

## 4. Conclusions

In this study, we derived the prediction equation of ground vibration by the linear regression analysis and analyzed the fragment size varying specific charge for the same scale of concrete foundation. We expressed the relationship between  $D_{av}$  and PPV using the relation between  $S_c$  and  $K$ , the relation between  $S_c$  and  $n$ , the relation between  $S_c$  and  $D_{av}$ .

As the relationship between  $S_c$  and  $K$  and  $S_c$  and  $n$ ,  $S_c$  is increased,  $K$  is increased but  $n$  is decreased. Also PPV is increased but  $D_{av}$  is decreased as the  $S_c$  is increased to demolish the equal volume concrete.

When the entire fragment volume of blasted concrete is equal, the  $D_{av}$  is increased because  $S_c$  and  $K$  are decreased and  $n$  is increased. When the  $D_{av}$  is constant, PPV is increased as the entire fragment volume of blasted concrete is increased.

Since ground vibration can be predicted through these linear relations, the effect of ground vibration to the surrounding environment and the fragment size can be considered at the same time when designing explosive demolition of concrete foundation.

### Acknowledgement

This study was carried out as a part of the high-tech urban development project of the Ministry of Land, Transport, and Maritime Affairs of Korea (Project No. 06 Construction Core B04).

### References

1) H. Park, R. H. Kim, C. G. Suk, and W. J. Jung, Conference of

- Korean Society for Rock Mechanics, 193–196, KSRM, Seoul, Korea (2010) (in Korean).
- 2) C. W. Lee, H. S. Yang, and S. G. Song, *EXPLOSIVE & BLASTING*, 18, 4(2000).
- 3) S. W. Choon, C. H. Ryu, and B. H. Choi, *EXPLOSIVE & BLASTING*, 19, 2(2001).
- 4) Y. K. Choi, C. I. Lee, J. S. Lee, and J. S. Kim, *TUNNEL & UNDERGROUND SPACE*, 14, 5(2004) (in Korean).
- 5) A. T. Spathis, Proc. 9<sup>th</sup> Int. Symp. On Rock Fragmentation by Blasting-FRAGBLAST 9, 209–219, Granada, Spain (2009).
- 6) S. P. Singh and R. Narendrula, Proc. 9<sup>th</sup> Int. Symp. On Rock Fragmentation by Blasting-FRAGBLAST 9, 311–317, Granada, Spain (2009).
- 7) H. Park, J. U. Song, and S. K. Kim, *EXPLOSIVE & BLASTING*, 23, 2(2005) (in Korean).
- 8) C. V. Cunningham, Proc. 1<sup>st</sup> Int. Symp. On Rock Fragmentation by Blasting, 439–453, Lulea, Sweden (1983).
- 9) A. Rustan, *International Journal of Blasting and Fragmentation*, 2(1998).